

Anomalies of upper critical field in the spinel superconductor

$\text{LiTi}_2\text{O}_{4-\delta}$

Zhongxu Wei,^{1,2,*} Ge He,^{1,2,*} Wei Hu,^{1,2,*} Jie Yuan,^{1,3} Chuanying Xi,⁴

Qian Li,^{1,3} Beiyi Zhu,^{1,3} Fang Zhou,^{1,2,3} Xiaoli Dong,^{1,2,3} Li Pi,⁴

Fedor V. Kusmartsev,^{5,6,7} Zhongxian Zhao,^{1,2,3} and Kui Jin^{1,2,3,†}

¹*Beijing National Laboratory for Condensed Matter Physics,*

Institute of Physics, Chinese Academy of Sciences, Beijing 100190, China.

²*School of Physical Sciences, University of Chinese Academy of Sciences, Beijing 100049, China.*

³*Songshan Lake Materials Laboratory, Dongguan, Guangdong 523808, China*

⁴*Anhui Province Key Laboratory of Condensed Matter Physics at Extreme Conditions, High Magnetic Field Laboratory of the Chinese Academy of Science, Hefei 230031, Anhui, China.*

⁵*Department of Physics, Loughborough University, Loughborough LE11 3TU, UK.*

⁶*Micro/Nano Fabrication Laboratory Microsystem and THz Research Center, Chengdu, Sichuan, China*

⁷*ITMO University, St. Petersburg 197101, Russia*

(Dated: July 21, 2022)

High-field electrical transport and point-contact tunneling spectroscopy were used to investigate superconducting properties of the unique spinel oxide, $\text{LiTi}_2\text{O}_{4-\delta}$ films with various oxygen content. We find that the upper critical field B_{c2} gradually increases as more oxygen impurities are brought into the samples by carefully tuning the deposition atmosphere. It is striking that although the superconducting transition temperature and energy gap are not changed, an astonishing isotropic B_{c2} up to ~ 26 Tesla is observed in oxygen-rich sample, which is almost doubled compared to the anoxic sample and breaks the Pauli limit. Such upper critical field anomalies were rarely reported in other three dimensional superconductors. Combined with all the anomalies, momentum dependent spin-orbit interaction induced by tiny oxygen impurities is naturally proposed to account for the remarkable enhancement of B_{c2} in oxygen-rich $\text{LiTi}_2\text{O}_{4-\delta}$ films. Such mechanism could be general and therefore provides ideas for optimizing practical superconductors.

PACS numbers: 74.25.Op, 71.70.Ej, 74.55.+v, 74.78.-w

* These authors contributed equally to this work.

† Corresponding author: kuijin@iphy.ac.cn

In conventional Bardeen-Cooper-Schrieffer (BCS) superconductors, time reversal and spatial inversion symmetries are essential to the formation of Cooper pairs[1]. An external field B violates the time reversal symmetry in a superconductor, thereby may break the Cooper pairs[2]. Superconductivity will be completely destroyed when B reaches an upper critical field B_{c2} for type-II superconductors. The underlying mechanisms that dominate and effectively increase B_{c2} intrigue intensive interests in condensed matter physics. Generally, B_{c2} is determined by orbit pair-breaking for conventional superconductors since spin susceptibility goes to zero at low temperatures[3]. In this case, B_{c2} can be enhanced by several factors that suppress orbit pair-breaking, such as narrow bands[4], short mean free path[5], and strong electron-phonon coupling[6]. Alternatively, spin flips induced by B will dominate B_{c2} when orbital effect is eliminated such as ultrathin Be[7] and Al films[8, 9] whose dimensionality is reduced. No matter which of aforementioned effects happens, B_{c2} is not expected to break the Clogston-Chandrasekhar limit[10, 11] or the Pauli paramagnetic limit B_P , where $B_P = 1.84T_c$ (in units of Tesla) for conventional superconductors and T_c is the superconducting transition temperature.

The upper critical field can be further enhanced and exceed B_P with some unconventional mechanisms where spin paramagnetism is crucial in the superconducting state, such as Fulde-Ferrell-Larkin-Ovchinnikov states[12–14], spin triplet pairing[15–17] and spin-orbit interaction[18–20]. In particular, spin-orbit interaction can give rise to two effects, i.e. spin-orbit coupling (SOC) and spin-orbit scattering (SOS). In the former case, the effect of spin flip can be weakened by locking spin parallel or perpendicular to in-plane due to Rashba SOC[1] or Zeeman SOC[3, 21], respectively. As for SOS, spin flip scattering will mix the different spin states and lead to a finite Pauli paramagnetism even at zero temperature thus enhancing B_{c2} [22]. Generally, the effects of spin-orbit interaction are prominent in low dimensional materials with non-centrosymmetry. However, it is rare to see the breaking of Pauli limit in conventional superconductors with centrosymmetry.

$\text{LiTi}_2\text{O}_{4-\delta}$ is a centrosymmetric conventional superconductor system with highly nontrivial spin-orbit structure[23]. For ideal LiTi_2O_4 structure, the valence of Ti is 3.5+ with low d -orbital filling and Jahn-Teller distortions, implying that large orbital freedom exists in this system[24]. Orbital order and spin-orbit scattering are unveiled in the anoxic films where amounts of ordering oxygen vacancies have been explicated[23, 25]. As the vacancies are gradually filled by introducing oxygen atoms, the orbital order is suppressed locally and spin-orbit scattering is enhanced at low temperatures[26]. Therefore, studying the evolution of B_{c2} of $\text{LiTi}_2\text{O}_{4-\delta}$ with various oxygen content may disclose some evidence and get further insight into the spin-orbit interaction in centrosymmetric superconductors.

In this letter, we present systematic transport measurements and point-contact tunneling spectroscopy study of $\text{LiTi}_2\text{O}_{4-\delta}$ films with various oxygen content. For oxygen-rich samples, a significantly enhanced B_{c2} up to 26 T at low temperature is observed. Furthermore, such nearly doubled B_{c2} compared with anoxic samples is isotropic. In fact, our data can be well fitted by the Werthamer-Helfand-Hohenberg (WHH) theory considering spin paramagnetism and spin-orbit scattering[27]. To our surprise, some other key parameters such as superconducting transition temperature T_c , superconducting energy gap Δ and electron-phonon coupling λ_{ep} are not changed. This is exactly what happens at spin-orbit scattering as described long ago by Gor'kov and Rusinov[28]. Here we show that the enhancement of B_{c2} is attributed to oxygen impurities which induces orbital moments and spin-orbit scattering centers. These orbital moments are created by the interplay between Jahn-Teller and spin-orbit effects on Ti sublattice.

High-quality $\text{LiTi}_2\text{O}_{4-\delta}$ thin films were epitaxially grown on MgAl_2O_4 (001) substrates by pulsed laser deposition under various oxygen pressures from basic vacuum ($< 1 \times 10^{-6}$ Torr) to $\sim 5 \times 10^{-6}$ Torr[26]. The temperature- and field-dependence of resistance were measured by a standard four-probe method in a commercial cryostat with field up to 16 T and temperature down to 2 K, and steady high magnetic field facility at High Magnetic Field Laboratory of Chinese Academy of Sciences with field up to 33 T. Point-contact measurements were performed by employing a homemade probe compatible with the 16 T commercial equipment. The point-contact junctions are established using Pt/Ir tips and the sample stage motion is allowed along both the x - and z -axes in range of 2.5 mm and 3 mm, respectively. The differential conductance dI/dV is measured by standard lock-in technique in quasi-four-probe configuration.

Fig. 1 (a) shows the resistance versus temperature curves for S_{oxy} and S_{vac} , deposited under oxygen pressure $\sim 5 \times 10^{-6}$ Torr and basic vacuum, respectively. Both samples display similar T_c of 11.25 ± 0.25 K with narrow transition widths of < 0.5 K, as seen in the inset of Fig. 1 (a). However, the residual resistance ratio (RRR), defined by room temperature resistance over resistance at 20 K ($R_{300\text{K}}/R_{20\text{K}}$), shows remarkable difference, i.e. 8.4 for S_{vac} and 2.3 for S_{oxy} . These results are consistent with our previous report[26]. The magnetic field-dependent resistance $R(B)$ isotherms of S_{vac} and S_{oxy} with field perpendicular to the ab -plane of films are shown in Fig. 1 (b) and (c), respectively. It is intriguing that the upper critical field B_{c2} of S_{oxy} is prominently enhanced compared with that of S_{vac} . Fig. 1 (d) and (e) show the corresponding $R(B)$ isotherms where the direction of magnetic field is parallel to the ab -plane.

In order to quantitatively study the enhancement of B_{c2} , we extract the temperature-dependent B_{c2} of S_{vac} and S_{oxy} with field parallel and perpendicular to ab -plane, as shown in Fig. 2 (a).

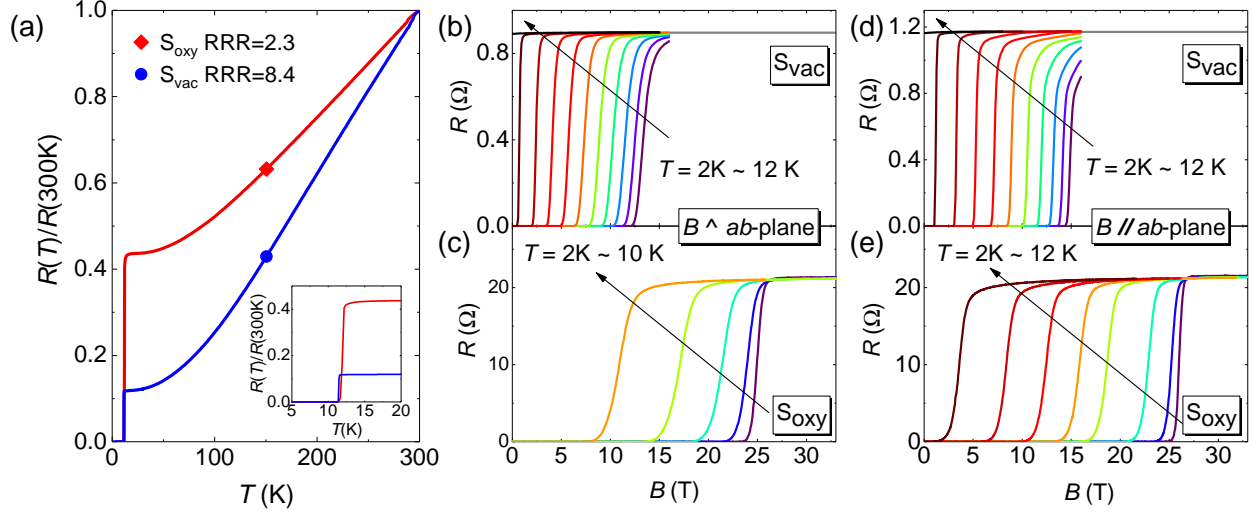


FIG. 1. **Temperature and magnetic field-dependent resistance of $\text{LiTi}_2\text{O}_{4-\delta}$ films.** (a) $R(T)$ curves of S_{oxy} (red line) and S_{vac} (blue line). They have similar T_c (~ 11 K) but different residual resistance ratio (RRR) where $\text{RRR} \equiv R_{300\text{K}}/R_{20\text{K}}$, i.e. $\text{RRR} = 2.3$ for S_{oxy} and $\text{RRR} = 8.4$ for S_{vac} . Inset: Zoom in of $R(T)$ curves. (b) $R(B)$ curves of S_{vac} from 2 K to 12 K with $\Delta T = 1$ K. (c) $R(B)$ curves of S_{oxy} from 2 K to 10 K with $\Delta T = 2$ K. The magnetic field is perpendicular to ab -plane of S_{vac} (b) and S_{oxy} (c). (d) $R(B)$ curves of S_{vac} from 2 K to 12 K with $\Delta T = 1$ K. (e) $R(B)$ curves of S_{oxy} at various temperatures. $T \in [2 \text{ K}, 8 \text{ K}]$ with $\Delta T = 2$ K; $T \in [9 \text{ K}, 12 \text{ K}]$ with $\Delta T = 1$ K. The magnetic field is parallel to the ab -plane of S_{vac} (d) and S_{oxy} (e). The grey lines in (b) and (d) are linearly extrapolated from experimental data.

The value of B_{c2} is evaluated at 90% of the resistance transition relative to the normal state resistance. It is found that the B_{c2} of S_{oxy} at 2 K is ~ 26 T, nearly doubled compared to that of S_{vac} . Furthermore, the B_{c2} of $\text{LiTi}_2\text{O}_{4-\delta}$ is isotropic since the values are almost unchanged no matter whether the field is applied along the ab -plane or out-of-plane. To get further insight into the isotropic enhancement of B_{c2} , we choose RRR as a good quantity to distinguish different samples since RRR monotonically decreases with increasing the oxygen pressure[26]. Fig . 2 (b) shows normalized temperature (T/T_c) dependence of B_{c2}/B_P for samples with different RRR. Two equations, i.e. $B_P = 1.84T_c$ and $B_P = \Delta/(\sqrt{2}\mu_B)$, can be used to calculate B_P , where μ_B is the Bohr magneton. Since the difference is small, i.e. < 3 T, we use the first expression to estimate B_P . Obviously, B_{c2}/B_P gradually increases as RRR decreases, and the B_{c2} of S_{oxy} exceeds B_P at low temperature. Typically, B_{c2}/B_P versus T/T_c of three selected samples with much different RRR (i.e. 8.4, 5.2, and 2.3) are fitted by the WHH theory in dirty limit[27]. The theoretical fits match well with experimental data, considering Maki parameter α and spin-orbit scattering λ_{so} [27, 29]. α and λ_{so} are approximately zero in the case of large RRR ($=8.4$) and increase monotonically

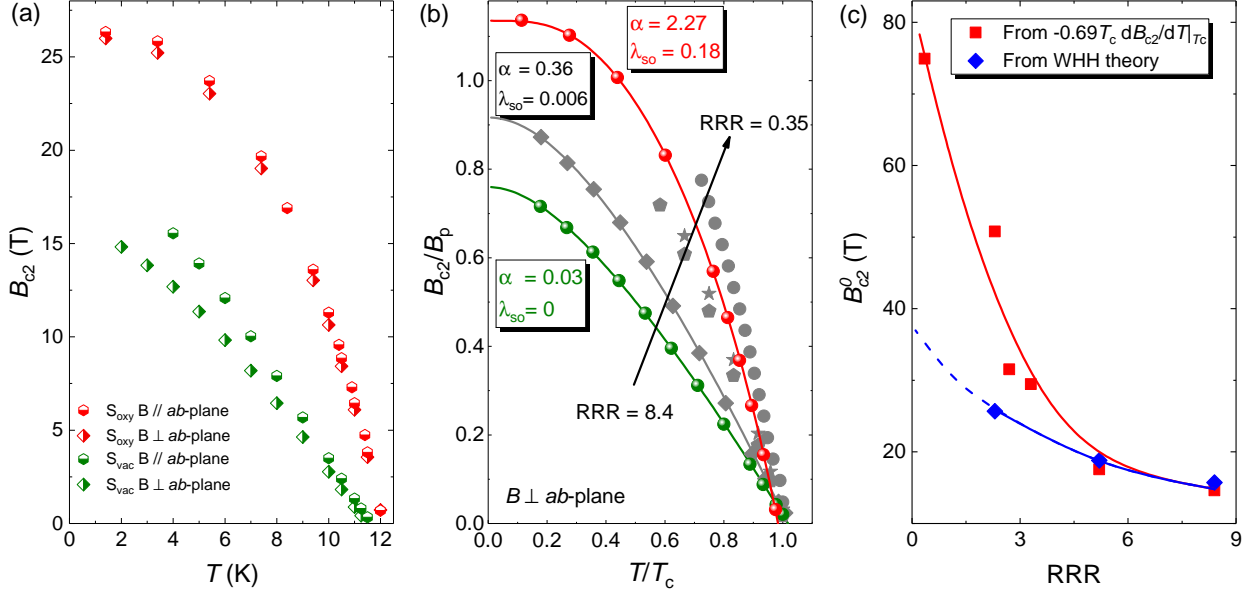


FIG. 2. **Upper critical field-temperature phase diagram of $\text{LiTi}_2\text{O}_{4-\delta}$ films.** (a) The temperature-dependent upper critical field B_{c2} of S_{oxy} and S_{vac} with field parallel and perpendicular to ab -plane respectively. The B_{c2} is evaluated at 90% of the resistive transition relative to the normal state resistance. (b) The temperature-dependent normalized upper critical field B_{c2}/B_p of series of $\text{LiTi}_2\text{O}_{4-\delta}$ films with RRR equal to 8.4, 5.2, 3.3, 2.7, 2.3 and 0.35. The applied field is perpendicular to ab -plane. The B_p is estimated by $1.84T_c$. Some of data are fitted by the WHH theory (solid lines). λ_{so} and α are fitting parameters of the WHH theory. (c) The upper critical field at zero temperature B_{c2}^0 values of these samples, which are estimated by $-0.69T_c(dB_{c2}/dT)|_{T_c}$ (red squares) and the WHH theory (blue diamonds) respectively. The solid and dash lines are to guide the eye.

with decreasing RRR, tempting us to consider spin paramagnetism and spin-orbit scattering for the enhanced B_{c2} . In addition, the zero-temperature upper critical field B_{c2}^0 extrapolated from the WHH theory is shown in Fig. 2 (c). A widely used formula which only considers orbital effect, $B_{c2}^0 = -0.69T_c(dB_{c2}/dT)|_{T_c}$, is also employed to estimate B_{c2}^0 , as shown in Fig. 2 (c). The difference in B_{c2}^0 by these two methods is small for samples with large RRR, while it becomes more and more prominent as RRR decreases, suggesting again that effects other than the orbital depairing should be considered for the B_{c2} anomalies.

To further clarify the key factors that lead to anomalies of B_{c2} , we carried out point-contact tunneling spectroscopy measurements for S_{oxy} whose RRR = 3.4. Fig. 3 (a) and (b) display the normalized temperature- and field-dependent tunneling spectra respectively, with B perpendicular to ab -plane. The differential conductance spectra clearly show a pair of superconducting coherence peaks, which are still robust against field up to 16 T at 2.5 K. All the spectra are fitted well

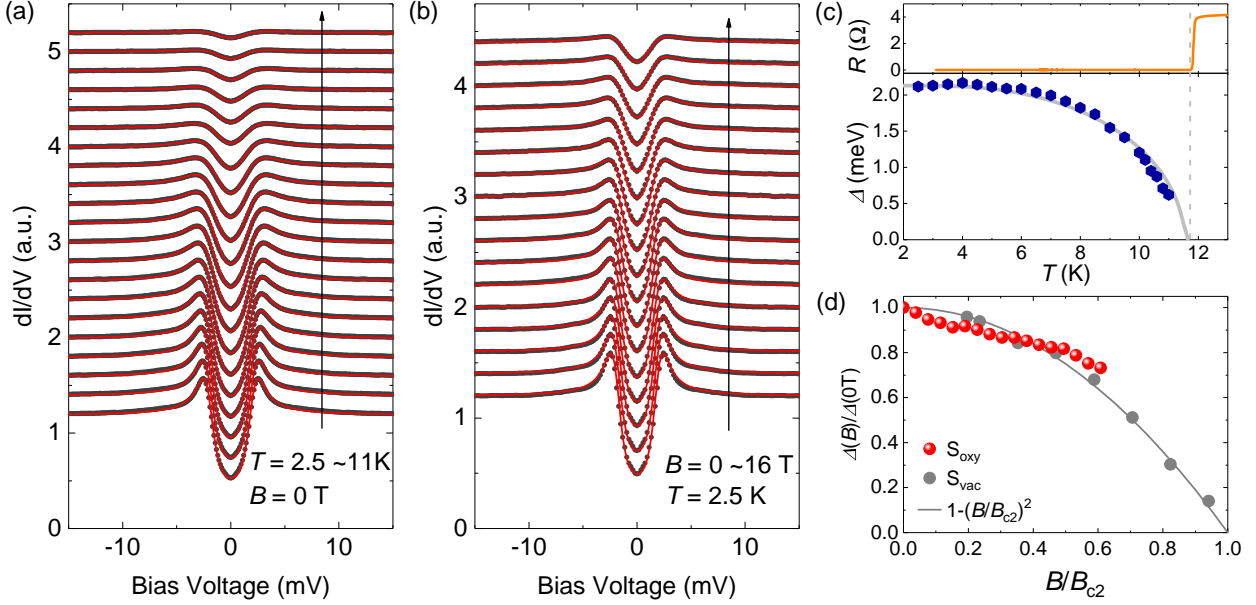


FIG. 3. **Temperature- and field-dependent tunneling spectra and the superconducting energy gap of S_{oxy} .** (a) Normalized differential conductance curves from 2.5 K to 10 K with $\Delta T = 0.5$ K and from 10.2 K to 11 K with $\Delta T = 0.2$ K in zero field. Experimental data (black dots) are fitted by the modified BTK model (red lines)[23]. All the data are vertically shifted for clarity. (b) Normalized differential conductance versus field from 0 T to 16 T with $\Delta B = 1$ T at 2.5 K. Experimental data (black dots) are also fitted by the modified BTK model (red lines). Data in fields are vertically shifted. (c) The top panel shows $R(T)$ curve of S_{oxy} . The temperature-dependent energy gap values (blue hexagons) shown in bottom panel are fitted by the BCS theory (grey line), and $2\Delta/k_{\text{B}}T_{\text{c}} = 4.2$. The vertical dash line indicates that the energy gap closing temperature is consistent with T_{c} . (d) Normalized energy gap versus $B/B_{\text{c}2}$ (red spheres). The normalized gap values of samples deposited in high vacuum (grey dots) are extracted from our previous work[23]. The grey line is plotted by the function, $\Delta(B)/\Delta(0T) = 1 - (B/B_{\text{c}2})^2$.

with the framework of Blonder-Tinkham-Klapwijk (BTK) model[23]. The barrier strength Z_{BTK} is $\sim 1.9 - 2.2$ at zero field, confirming that our point-contact measurements are in the tunneling limit[23]. The temperature-dependent superconducting energy gap $\Delta(T)$ obtained from the BTK fits, agrees well with BCS theory and $2\Delta/k_{\text{B}}T_{\text{c}} = 4.2$ where k_{B} is the Boltzmann constant, as shown in the bottom panel of Fig. 3 (c). Compared with S_{vac} , the $2\Delta/k_{\text{B}}T_{\text{c}}$ of S_{oxy} is nearly unchanged[23, 25], indicating that the electron-phonon coupling λ_{ep} remains the same. However, the normalized field-dependent energy gap $\Delta(B)/\Delta(0)$ of S_{oxy} versus B deviates from the relation, $\Delta(B)/\Delta(0) = 1 - (B/B_{\text{c}2})^2$, which is discovered in S_{vac} [23], as shown in Fig. 3 (d). This unusual behavior of $\Delta(B)$ suggests that orbital order is suppressed while spin-orbit scattering might be enhanced in S_{oxy} , coinciding with our previous work[26].

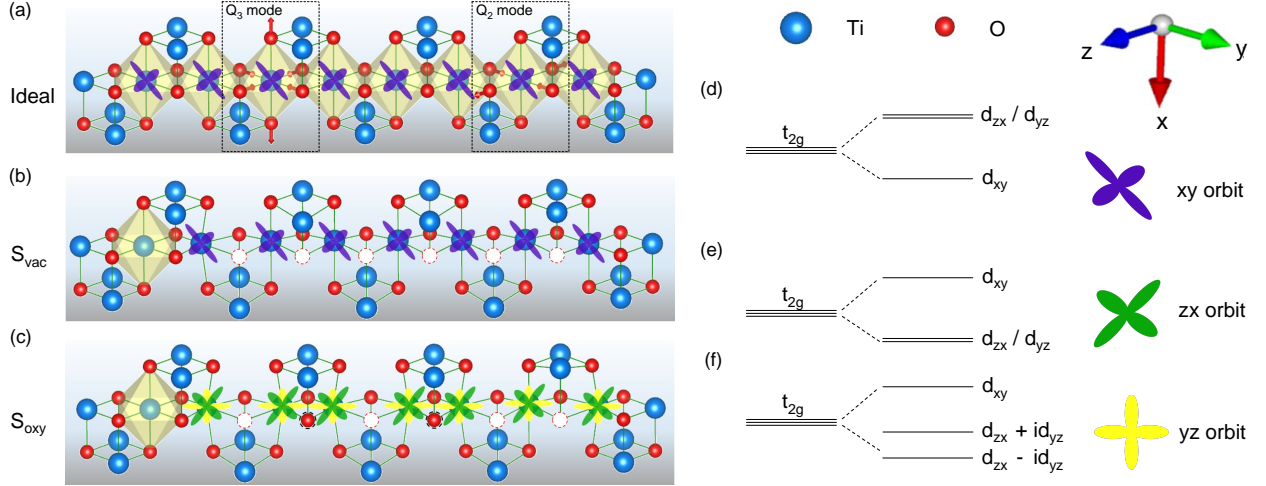


FIG. 4. **The crystal structures and proposed band splitting of $\text{LiTi}_2\text{O}_{4-\delta}$.** (a) Octahedron chain in ideal LiTi_2O_4 structure. The red arrows show the phonon vibration modes, i.e. Q_2 and Q_3 modes. d_{xy} orbitals are shown in the Ti atoms. (b) Octahedron chain in S_{vac} . The dotted circles stand for the oxygen vacancies. d_{xy} orbitals are shown in the Ti atoms. (c) Octahedron chain in S_{oxy} . The oxygen atoms surrounded by dotted circles stand for the filled oxygen vacancies. $d_{zx} + id_{yz}$ and $d_{zx} - id_{yz}$ are shown in the Ti atoms. (d) Orbital level splitting induced by Jahn-Teller distortion in ideal LiTi_2O_4 structure and S_{vac} . (e) Orbital level splitting induced by Jahn-Teller distortion with the existence of oxygen impurities. (f) Orbital level splitting induced by Jahn-Teller distortion and spin-orbit coupling in S_{oxy} .

Now let's turn to discuss the mechanism behind the enhancement of B_{c2} for $\text{LiTi}_2\text{O}_{4-\delta}$ films. Firstly, some aforementioned factors can be easily ruled out. Dimensionality effect is only considered when the sample thickness is comparable with the lattice constant, while the thickness of our samples is larger than 70 nm. Zeeman SOC and Rashba SOC can be excluded because the lattice structure of $\text{LiTi}_2\text{O}_{4-\delta}$ is centrosymmetric and B_{c2} is isotropic[3, 21]. In addition, the orbital depairing effect is suppressed since α in S_{oxy} is significantly enhanced[27, 29]. However, the electron effective mass derived from the excellent WHH fitting increases with increasing RRR, indicating that anoxic samples have a narrower band, thereby the effect of narrow band is also excluded[30]. In order to verify whether the effect of mean free path is dominant, we can calculate the relaxation time τ by a formula based on the WHH theory, i.e. $\tau = 3\hbar/(4E_{\text{F}}^{\text{vac}}\alpha)$ where \hbar and $E_{\text{F}}^{\text{vac}}$ are the reduced Planck constant and Fermi energy of S_{vac} respectively. The τ of S_{vac} is equal to 3.8×10^{-14} s, which is self-consistent with the result derived from electrical transport, i.e. $\tau = l/v_{\text{F}} = 1.3 \times 10^{-14}$ s, where l is mean free path and v_{F} is Fermi velocity[23]. However, the excellent fitting of S_{oxy} provides an underestimation of τ ($= 5 \times 10^{-16}$ s) if we assume its Fermi energy E_{F} equals to $E_{\text{F}}^{\text{vac}}$, since such τ is even smaller than the lower limit τ_{min} ($= c/v_{\text{F}} = 6.1 \times 10^{-15}$ s),

restricted by the Mott-Ioffe-Regel limit[26, 31]. Here c is the out-of-plane lattice constant. Nevertheless, such confliction can be reconciled in case of a reduced $E_F \sim E_F^{vac}/8$. It is surprising that tiny amount of oxygen defects can induce such remarkable change in Fermi energy unless the occurrence of Fermi surface reconstruction[32] or Lifshitz transition[33] and formation of small Fermi pockets, like in cuprates[32]. We expect that such variation of Fermi energy should have influence on density of states thereby tuning T_c and Δ , which is not observed in our work since a higher oxygen pressure will trigger a phase transition from $\text{LiTi}_2\text{O}_{4-\delta}$ to $\text{Li}_4\text{Ti}_5\text{O}_{12}$ [26]. Therefore, some effects beyond the WHH theory we used should be also taken into account such as strong electron-phonon coupling[34] and clean limit[5]. The former case can be naturally ruled out by the small value of electron-phonon coupling $\lambda_{ep} \sim 0.65$ [35, 36] and the almost unchanged $2\Delta/(k_B T_c)$. The clean limit is not suitable for $\text{LiTi}_2\text{O}_{4-\delta}$ since $l \ll \xi$, where ξ is coherence length[23].

Up to now, we haven't considered the effect of spin-orbit scattering, since the values of λ_{so} derived from our fitting are too small to induce such large enhancement of B_{c2} compared with other systems[5]. In the WHH theory, s -wave scattering is assumed, while other factors like the details of spin-orbit interaction are ignored[27, 34], which may also play an essential role in the anomalies of B_{c2} . In order to clarify this issue, we consider the connection between the crystal structures and spin-orbit interaction in three configurations, i.e. ideal LiTi_2O_4 structure (see Fig. 4 (a)), existence of long range ordered oxygen vacancies (S_{vac} , see Fig. 4 (b)) and the case where these vacancies are partially filled by oxygen atoms (S_{oxy} , see Fig. 4 (c)). Since it is impossible to take into account oxygen impurities with random distribution in band structure calculations, we would like to discuss it phenomenologically. For the ideal LiTi_2O_4 structure, Jahn-Teller distortions with Q_2 and Q_3 modes exist homogeneously[37]. In this case, the compression of TiO_6 octahedron dominates, and t_{2g} orbitals split into higher two-fold degenerate d_{zx}/d_{yz} and lower non-degenerate d_{xy} [38] (see Fig. 4 (d)). If long range ordered oxygen vacancies exist (S_{vac}), such distortion will be stabilized ($c/a \sim 0.99$, where a is the in-plane lattice constant), and orbital-related state is expected to form, which is indeed observed in S_{vac} [23, 26]. Here on the single octahedron the orbital moment of the conduction electron quenches out.

However, spin-orbit interaction should be taken into account even if only one oxygen vacancy is filled since the gradient of local electrical potential V cannot be neglected. In general, the Hamiltonian term of SOC can be expressed as

$$H_{soc} = \lambda_{soc}(\nabla V \times \mathbf{k}) \cdot \boldsymbol{\sigma} , \quad (1)$$

where λ_{soc} is the spin-orbit coupling constant, \mathbf{k} is the momentum of the conduction electron,

σ is the Pauli matrix[39]. It is well known that λ_{soc} strongly increases with the atomic number Z , i.e. $\lambda_{\text{soc}} \sim Z^4$ [40]. In this case, the energy scale of SOC is comparable to that of Jahn-Teller distortions[40, 41]. Therefore, the SOC competes with the Jahn-Teller effect and leads to a reversal of orbital splitting, i.e. higher non-degenerate d_{xy} and lower two-fold degenerate d_{zx}/d_{yz} [42](see Fig. 4 (e)). Typically, the SOC overbears the types of Jahn-Teller distortion, and further splits two-fold degenerate d_{zx}/d_{yz} into $d_{zx} + id_{yz}$ and $d_{zx} - id_{yz}$ (see Fig. 4 (f)), consequently generating an orbital moment quantum number $l = \pm 1$. As a result, when an external magnetic field B is applied, the effective field B_{eff} is given by

$$B_{\text{eff}} = B + \langle B_{\text{soc}} \rangle , \quad (2)$$

where $\langle B_{\text{soc}} \rangle$ is the average value of the generated SOC field. Since $\langle B_{\text{soc}} \rangle$ is negative due to the opposite orientations of orbital moment and spin, the external field is weakened and thus the B_{c2} is enhanced. The similar situation with the orbital moment orientations has been discussed in another Ti oxide compound LaTiO_3 , which has a similar ordering of orbital energies[43, 44].

Momentum-dependent spin-orbit scattering may also contribute to such enhancement of B_{c2} in S_{oxy} . Other anomalies can be well understood in this framework. Firstly, due to the nonselective distribution of oxygen impurities, such scattering is isotropic in average, leading to an isotropic B_{c2} . Secondly, such spin-orbit interaction has no effect on the thermodynamics of a superconductor, especially T_c , pointed out by Gor'kov and Rusinov[28], which is consistent with our results. Thirdly, the deviation from $\Delta(B) \sim -B^2$ in S_{oxy} indicates the suppression of orbital order via the randomly oriented and distributed orbital moments, therewith the enhanced spin-orbit scattering. It is established that such spin-orbit interaction plays a key role in the band inversion of topological materials[45–47], Ising superconductivity[21, 48], the vortex phase transition from liquid to solid[49], breaking the Pauli limit of (quasi) two dimensional superconductors[20, 50] and so on.

Overall, by a systematic transport and point-contact tunneling spectroscopy measurements of the $\text{LiTi}_2\text{O}_{4-\delta}$ films we find an astonishing enhancement of the B_{c2} , that breaks the Pauli limit and meanwhile remains isotropic. Such anomalies are rarely observed in superconductors with cubic structure, yet the breaking of the Pauli limit is frequently reported in (quasi) two dimensional non-centrosymmetric superconducting materials but with an anisotropic B_{c2} . Moreover, oxygen impurities, giving rise to higher residual resistivity, do not make obvious influence on T_c and Δ . In combination with our previous work on this system[23, 26], we conclude that the three dimensional spin-orbit interaction induced by oxygen impurities is essential to the significant isotropic enhancement of B_{c2} . The effects of oxygen impurities could be general, thus it is tempting to verify

such effects in other transition metal oxides. In addition, our achievements pave a promising path to optimize practical superconductors with higher upper critical field.

We thank X. Zhang, J. S. Zhang for fruitful discussions. This work was supported by the National Key Basic Research Program of China (2015CB921000, 2017YFA0303003, 2017YFA0302902 and 2018YFB0704102), the National Natural Science Foundation of China (11674374 and 11804378), the Key Research Program of Frontier Sciences, CAS (QYZDB-SSW-SLH008 and QYZDY-SSW-SLH001), the Key Research Program of the Chinese Academy of Sciences (XDPB01). The work of F.V.K. was supported by the Government of the Russian Federation through the ITMO Professorship Program. A portion of this work was performed on the Steady High Magnetic Field Facilities, High Magnetic Field Laboratory, CAS.

-
- [1] E. Bauer and M. Sigrist, *Non-Centrosymmetric Superconductors* (Springer, 2012).
 - [2] D. Saint-James, G. Sarma, and E. J. Thomas, *Type II Superconductivity* (Pergamon Press, Oxford, 1969).
 - [3] E. Sohn, X. Xi, W. Y. He, S. Jiang, Z. Wang, K. Kang, J. H. Park, H. Berger, L. Forró, K. T. Law, J. Shan, and K. F. Mak, *Nat. Mater.* **17**, 504 (2018).
 - [4] K. Holczer, O. Klein, G. Grüner, J. D. Thompson, F. Diederich, and R. L. Whetten, *Phys. Rev. Lett.* **67**, 271 (1991).
 - [5] Ø. Fischer, *Appl. Phys.* **16**, 1 (1978).
 - [6] T. P. Orlando, E. J. McNiff, S. Foner, and M. R. Beasley, *Phys. Rev. B* **19**, 4545 (1979).
 - [7] P. W. Adams, P. Herron, and E. I. Meletis, *Phys. Rev. B* **58**, R2952 (1998).
 - [8] P. M. Tedrow and R. Meservey, *Phys. Rev. B* **25**, 171 (1982).
 - [9] R. Meservey and P. M. Tedrow, *Phys. Rep.* **238**, 173 (1994).
 - [10] A. M. Clogston, *Phys. Rev. Lett.* **9**, 266 (1962).
 - [11] B. S. Chandrasekhar, *Appl. Phys. Lett.* **1**, 7 (1962).
 - [12] P. Fulde and R. A. Ferrell, *Phys. Rev.* **135**, A550 (1964).
 - [13] A. I. Larkin and Y. N. Ovchinnikov, *JETP* **20**, 762 (1965).
 - [14] Y. Matsuda and H. Shimahara, *J. Phys. Soc. Jpn.* **76**, 051005 (2007).
 - [15] D. Aoki, A. Huxley, E. Ressouche, D. Braithwaite, J. Flouquet, J. P. Brison, E. Lhotel, and C. Paulsen, *Nature* **413**, 613 (2001).
 - [16] N. T. Huy, A. Gasparini, D. E. de Nijs, Y. Huang, J. C. P. Klaasse, T. Gortenmulder, A. de Visser, A. Hamann, T. Görlach, and H. v. Löhneysen, *Phys. Rev. Lett.* **99**, 067006 (2007).
 - [17] D. Aoki and J. Flouquet, *J. Phys. Soc. Jpn.* **81**, 011003 (2012).
 - [18] A. A. Abrikosov and L. P. Gor'kov, *JETP* **15**, 752 (1962).

- [19] R. Meservey, P. M. Tedrow, and R. C. Bruno, *Phys. Rev. B* **11**, 4224 (1975).
- [20] X. S. Wu, P. W. Adams, Y. Yang, and R. L. McCarley, *Phys. Rev. Lett.* **96**, 127002 (2006).
- [21] J. M. Lu, O. Zheliuk, I. Leermakers, N. F. Q. Yuan, U. Zeitler, K. T. Law, and J. T. Ye, *Science* **350**, 1353 (2015).
- [22] K. Maki and T. Tsuneto, *Prog. Theor. Phys.* **31**, 945 (1964).
- [23] K. Jin, G. He, X. Zhang, S. Maruyama, S. Yasui, R. Suchoski, J. Shin, Y. Jiang, H. S. Yu, J. Yuan, L. Shan, F. V. Kusmartsev, R. L. Greene, and I. Takeuchi, *Nat. Commun.* **6**, 7183 (2015).
- [24] S. Satpathy and R. M. Martin, *Phys. Rev. B* **36**, 7269 (1987).
- [25] G. He, Y. Jia, X. Hou, Z. Wei, H. Xie, Z. Yang, J. Shi, J. Yuan, L. Shan, B. Zhu, H. Li, L. Gu, K. Liu, T. Xiang, and K. Jin, *Phys. Rev. B* **95**, 054510 (2017).
- [26] Y. Jia, G. He, W. Hu, H. Yang, Z. Yang, H. Yu, Q. Zhang, J. Shi, Z. Lin, J. Yuan, B. Zhu, L. Gu, H. Li, and K. Jin, *Sci. Rep.* **8**, 3995 (2018).
- [27] N. R. Werthamer, E. Helfand, and P. C. Hohenberg, *Phys. Rev.* **147**, 295 (1966).
- [28] L. P. Gor'kov and A. I. Rusinov, *JETP* **19**, 922 (1964).
- [29] K. Maki, *Physics* **1**, 127 (1964).
- [30] G. R. Stewart, *Rev. Mod. Phys.* **56**, 755 (1984).
- [31] N. E. Hussey, K. Takenaka, and H. Takagi, *Philos. Mag.* **84**, 2847 (2004).
- [32] H. Matsui, T. Takahashi, T. Sato, K. Terashima, H. Ding, T. Uefuji, and K. Yamada, *Phys. Rev. B* **75**, 224514 (2007).
- [33] I. M. Lifshitz, *JETP* **11**, 1130 (1960).
- [34] C. T. Rieck, K. Scharnberg, and N. Schopohl, *J. Low Temp. Phys.* **84**, 381 (1991).
- [35] S. Massidda, J. J. Yu, and A. J. Freeman, *Phys. Rev. B* **38**, 11352 (1988).
- [36] C. P. Sun, J. Y. Lin, S. Mollah, P. L. Ho, H. D. Yang, F. C. Hsu, Y. C. Liao, and M. K. Wu, *Phys. Rev. B* **70**, 054519 (2004).
- [37] H. C. Longuethiggins, U. Öpik, M. H. L. Pryce, and R. A. Sack, *Proc. Royal Soc. Lond.* **244**, 1 (1958).
- [38] D. I. Khomskii and T. Mizokawa, *Phys. Rev. Lett.* **94**, 156402 (2005).
- [39] L. H. Thomas, *Nature* **117**, 514 (1926).
- [40] M. Watkins, A. Mainwood, and G. Davies, *Diam. Relat. Mater.* **12**, 503 (2003).
- [41] M. W. Haverkort, Z. Hu, A. Tanaka, G. Ghiringhelli, H. Roth, M. Cwik, T. Lorenz, C. Schüßler-Langeheine, S. V. Streltsov, A. S. Mylnikova, V. I. Anisimov, C. de Nadai, N. B. Brookes, H. H. Hsieh, H. J. Lin, C. T. Chen, T. Mizokawa, Y. Taguchi, Y. Tokura, D. I. Khomskii, and L. H. Tjeng, *Phys. Rev. Lett.* **94**, 056401 (2005).
- [42] I. B. Bersuker, *The Jahn-Teller effect* (Cambridge University Press, Cambridge, 2006).
- [43] T. Mizokawa and A. Fujimori, *Phys. Rev. B* **54**, 5368 (1996).
- [44] G. I. Meijer, W. Henggeler, J. Brown, O. S. Becker, J. G. Bednorz, C. Rossel, and P. Wachter, *Phys. Rev. B* **59**, 11832 (1999).
- [45] F. V. Kusmartsev and A. M. Tsel'vik, *JETP* **42**, 257 (1985).

- [46] D. Pesin and L. Balents, [Nat. Phys.](#) **6**, 376 (2010).
- [47] V. Galitski and I. B. Spielman, [Nature](#) **494**, 49 (2013).
- [48] B. T. Zhou, N. F. Q. Yuan, H. L. Jiang, and K. T. Law, [Phys. Rev. B](#) **93**, 180501 (2016).
- [49] A. I. Rykov, S. Tajima, F. V. Kusmartsev, E. M. Forgan, and C. Simon, [Phys. Rev. B](#) **60**, 7601 (1999).
- [50] R. A. Klemm, A. Luther, and M. R. Beasley, [Phys. Rev. B](#) **12**, 877 (1975).
- [51] G. E. Blonder, M. Tinkham, and T. M. Klapwijk, [Phys. Rev. B](#) **25**, 4515 (1982).